IEEE Access
Multidisciplinary | Rapid Review | Open Access Journal

Received August 17, 2017, accepted November 16, 2017, date of publication December 4, 2017,
date of current version December 22, 2017.

Digital Object Identifier 10.1109/ACCESS.2017.2777005

Comparison of Feedforward Synchronization Schemes for Full-Response CPM Signals

XU XIE[1] (Member, IEEE) AND ZHENGGUANG XU[2]
[1]PLA Naval University of Engineering, Wuhan 430015, China
[2]Huazhong University of Science and Technology, Wuhan 430073, China

Corresponding author: Zhengguang Xu (xray@mail.hust.edu.cn)

This work was supported in part by the National Natural Science Foundation of China under Grant 61501195 and in part by Naval University of Engineering under Grant HGDYDJJ13008.

ABSTRACT We compare three non-data-aided synchronization techniques for full-response continuous phase modulation (CPM) signals, which have feedforward structures and are suitable for burst-mode transmissions. All the schemes are based on the statistical characteristics of the full-response CPM signals with modulation index $h = 1$, for which the algorithms are investigated to estimate the carrier frequency offset, carrier phase, and symbol timing. For the CPM signal with an arbitrary modulation index, the phase unwrapping technique is used to convert the modulation index into 1, and then, the proposed algorithms could work. The performances of the synchronization algorithms are investigated by simulations and compared with the modified Cramer–Rao bounds. It turns out that the estimation performances of the frequency offset and timing offset are close to the theoretical limits in high signal-to-noise ratio.

INDEX TERMS Synchronization, frequency estimation, timing recovery, continuous phase modulation.

I. INTRODUCTION

Continuous phase modulation (CPM) is a bandwidth efficient digital modulation scheme used for data transmission over band-limited channels [1]. The transmitted symbol information is contained in the signal phase, so the CPM signal has the constant envelope, which allows simple transmitters and high efficiency in converting limited mobile power into radiated power [2]. In order to demodulate the CPM signal, the synchronization process is necessary. The synchronization procedure includes carrier recovery and timing recovery, and there are many research works on the issues [3].

The synchronization schemes can be divided into data-aided and non-data-aided schemes. In [4] and [5], the data-aided schemes are investigated and the recovery performance is close to the modified Cramer-Rao bound (MCRB) [6], but the training sequence must be inserted into the transmitted sequence so that the spectral efficiency decreases. Therefore, more research works focus on the non-data-aided schemes where the schemes could be divided into decision-feedback and feedforward structures. The decision-feedback scheme utilizes the symbol decision results to help the synchronization procedure where the synchronization step and demodulation step compose the feedback loop. The feedforward scheme is the open loop and the synchronization procedure is implemented independently with demodulation results. Therefore, the structure of the feedforward scheme is simpler than that of the feedback scheme. In our paper, we mainly consider the feedforward scheme.

The carrier recovery and timing recovery are independently investigated in some works. In [7], the frequency detectors for MSK-type signals is proposed when the timing recovery has been implemented for the received signals, where the MSK-type signal is the CPM signal with modulation index $h = 1/2$ since the minimum shift keying (MSK) is the mostly used CPM signal with $h = 1/2$. In [8]–[10], the timing recovery schemes are designed for CPM signals when the carrier frequency offset has been estimated.

When the CPM signal is received, both of the frequency offset and the symbol timing are unknown. Therefore, the frequency detector without the timing information or the timing recovery without frequency information is more attractive. The research works mainly focus on the CPM signals with $h = 1/2$ or MSK-type signals, which have some special characteristics for easy implementation. In [11], the frequency detectors for CPM signals with modulation index $h = 1/2$ are investigated, which can work without the timing information. The scheme decomposes the CPM signals into the superposition of pulse amplitude modulated (PAM) signals by Laurent's representation of CPM schemes [12], and then utilizes the maximum likelihood (ML) estimation method

2169-3536 © 2017 IEEE. Translations and content mining are permitted for academic research only.
Personal use is also permitted, but republication/redistribution requires IEEE permission.
See http://www.ieee.org/publications_standards/publications/rights/index.html for more information.

to obtain the carrier frequency. However, it is difficult to extend the algorithm to other h values, since the Laurent's representation is complex in general cases. In [13], the joint frequency and timing estimator is proposed for continuous phase frequency shift keying (CPFSK) signals with $h = 1$. The scheme constructs the objective function about the frequency and timing offsets and searches the peak of the function. When the peak is found, the frequency and timing offsets have been obtained. In [14] and [15], the joint estimator is proposed for MSK-type signals, the estimator utilizes the correlation function of the signal with the symbol period interval. In [16] and [17], another joint estimator is proposed for CPFSK signals, which converts the CPFSK signals with arbitrary h values into those with $h = 1$ by phase unwrapping and then estimates the frequency and timing offsets.

Comparing the schemes in [13]–[17], we could find the common viewpoint that all the algorithms use the characteristics of the CPM signals with $h = 1$. In [13], the algorithm is designed for the CPM signal with $h = 1$. In [14] and [15], the square operation is used to convert $h = 1/2$ into $h = 1$. In [16] and [17], the phase unwrapping algorithm is used to convert the arbitrary h values into $h = 1$. The basic principles for the three kinds of schemes are different. The cyclostationary properties of the CPM signals in [18] reveal the theoretical foundation for the schemes in [16] and [17], but the formulas in [18] are too complex to read.

In the paper, we summarize the statistical characteristics of the CPM signal with $h = 1$, and generalize these schemes to the general CPM signal. For simplicity, we restrict ourselves to full-response CPM [19], i.e., those with pulse length equal to the symbol period. Extensions to other pulse length are possible but, for space limitations, are not pursued here.

The paper is organized as follows. In Section II, we describe the statistical characteristics of CPM with $h = 1$ and provide the brief proofs. In Section III, we derive the joint estimators from the characteristics respectively. The numerical results are provided in Section IV and conclusions are summarized in Section V.

II. STATISTICAL CHARACTERISTICS OF THE CPM

The complex envelope of the CPM is

$$s(t) = \exp[j\phi(t)] \tag{1}$$

where the modulated phase is [1]

$$\phi(t) = 2\pi h \sum_{k=0}^{n} \alpha_k q(t - kT). \tag{2}$$

In the phase definition, h is the modulation index, T is the symbol period, and α_k are independent M-ary data symbols, each taking one of the values

$$\alpha_k = \pm 1, \pm 3, \cdots, \pm M - 1 \tag{3}$$

with equal probability $1/M$. Therefore, we have

$$E\{\alpha_k\} = 0. \tag{4}$$

Here $E\{\cdot\}$ denotes expectation operation to α_k. The function $q(t)$ is the phase pulse of the modulator, which is related to the frequency pulse $g(t)$ by the relationship

$$q(t) = \int_{-\infty}^{t} g(\tau)\, d\tau. \tag{5}$$

For full-response CPM signals, $g(t)$ is time-limited to the interval $(0, T)$ and satisfies $g(t) = g(T - t)$. Therefore,

$$q(t) = \begin{cases} 0, & t \le 0; \\ 1/2 - q(T - t), & 0 < t < T; \\ 1/2, & t \ge T. \end{cases} \tag{6}$$

Usually we consider two frequency pulses: rectangular pulse (REC) and raised-cosine (RC) pulse as follows.

$$g(t) = \frac{1}{2T}, \quad \text{with REC}, \tag{7}$$

$$g(t) = \frac{1}{2T}\left(1 - \cos\frac{2\pi t}{T}\right), \quad \text{with RC}. \tag{8}$$

which are both time-limited to the interval $(0, T)$.

For $h = 1$ and $M = 2$, the full-response CPM signals have following three statistical characteristics:

(i) $s(nT) = (-1)^n$;

(ii) $\mu(t) = E\{s(t)\}$ is a periodic function of time with period $2T$;

(iii) $r_m(t) = E\{s(t)\, s^*(t - mT)\}$ is a periodic function of time with period T.

Now we provide the brief proof. Extensions to other M values are possible but are not pursued here.

(i) We calculate the sample point at $t = nT$ as follows

$$s(nT) = \exp\left[j\pi \sum_{k=0}^{n-1} \alpha_k\right] = (-1)^n. \tag{9}$$

where $\exp(j\pi) = -1$ and $\sum_{k=0}^{n-1} \alpha_k$ is an integer. Since α_k is odd integer and $\sum_{k=0}^{n-1} \alpha_k$ is the sum of n odd integers, the parity of $\sum_{k=0}^{n-1} \alpha_k$ is the same as the parity of n. Therefore, we have $s(nT) = (-1)^n$.

The property is about the special samples of the CPM signals, so we call it as the sample point property.

(ii) We calculate the expectation of $s(t)$ as follows

$$\begin{aligned} \mu(t) &= E\left\{\exp\left[j2\pi \sum_{k=0}^{n} \alpha_k q(t - kT)\right]\right\} \\ &= \prod_{k=0}^{n} E\{\exp[j2\pi\alpha_k q(t - kT)]\} \\ &= \prod_{k=0}^{n} \cos 2\pi q(t - kT) \end{aligned} \tag{10}$$

where the properties

$$E\{\cos\alpha_k t\} = E\{\cos t\} = \cos t$$

$$E\{\sin\alpha_k t\} = E\{\alpha_k \sin t\} = 0$$

are used for $\alpha_k = \pm 1$. According to (6), we have

$$\mu(t) = (-1)^n \cos 2\pi q(t - nT), \quad nT \le t < (n+1)T. \tag{11}$$

It is easily seen that

$$\mu(t) = -\mu(t+T) = \mu(t+2T) \tag{12}$$

so that $\mu(t)$ can be expanded in the Fourier series form with period $2T$ as follows

$$\mu(t) = \sum_{m=-\infty}^{\infty} c_m e^{jm\pi t/T}. \tag{13}$$

Obviously, $c_m \neq 0$ for odd m and $|c_1| = |c_{-1}| > |c_m|$ $(m \neq \pm 1)$.

The property is about the mean function of the CPM signals, so we call it as the mean function property.

(iii) We calculate the correlation function of $s(t)$ similarly

$$\begin{aligned} r_m(t) &= E\left[s(t)\, s^*(t - mT)\right] \\ &= E\left\{\exp\left[j2\pi \sum_{k=0}^{n} \alpha_k p_m(t - kT)\right]\right\} \\ &= \prod_{k=0}^{n} \cos 2\pi p_m(t - kT) \end{aligned} \tag{14}$$

where m is an integer and

$$p_m(t) = q(t) - q(t - mT). \tag{15}$$

Considering the pulse $p_m(t)$ is time-limited to the interval $(0, (m+1)T)$, we have

$$p_m(t) = \begin{cases} q(t), & 0 < t < T; \\ 1/2, & T < t < mT; \\ 1/2 - q(t - mT), & mT < t < (m+1)T; \\ 0, & others. \end{cases} \tag{16}$$

Therefore, only m+1 items are available in (14). In the interval $nT < t < (n+1)T$,

$$\begin{aligned} r_m(t) &= \prod_{k=n-m}^{n} \cos 2\pi p_m(t - kT) \\ &= (-1)^m \cos^2 2\pi q(t - nT). \end{aligned} \tag{17}$$

According to (6),

$$r_m(t) = r_m(t+T). \tag{18}$$

Obviously, $r_m(t)$ is the even function with period T and the parameter m is just involved in $(-1)^m$. The item $\cos^2 2\pi q(t - nT)$ can be expanded in the Fourier series form as follows

$$\cos^2 2\pi q(t - nT) = A_0 + 2\sum_{k=1}^{\infty} A_k \cos\left(\frac{2\pi kt}{T}\right).$$

According to (17), we have the inference about $r_m(t)$ as follows

$$|r_m(t)| = A_0 + 2\sum_{k=1}^{\infty} A_k \cos\left(\frac{2\pi kt}{T}\right). \tag{19}$$

The property is about the correlation function of the CPM signals, so we call it as the correlation function property.

Above all, the three characteristics are proved. From the three properties, the information of the transmitted symbol is eliminated, so they could be used to estimate the frequency offset and timing offset. In fact, the sample point property is the foundation of the scheme in [13]. The mean function property is a special case of the cyclic spectral characteristic in [18], which is the foundation of the scheme in [16] and [17]. The correlation function property is the foundation of the scheme in [14] and [15]. In the next section, we derive three different synchronization schemes from the three properties respectively.

III. SYNCHRONIZATION SCHEMES FOR CPM SIGNALS

The complex envelope of the CPM signal with the frequency offset and timing offset is

$$x(t) = \exp[j(2\pi vt + \theta)]\, s(t - \tau) \tag{20}$$

where v is the frequency offset, θ is the carrier phase and τ is the timing offset. The three parameters are unknown, so the synchronization algorithms are designed to estimate the parameters. Now we provide three schemes from the three characteristics described in the last section.

A. SYNCHRONIZATION SCHEME FROM THE SAMPLE POINT PROPERTY

Substituting (9) into (20) yields

$$x(nT + \tau) = (-1)^n \exp[j(2\pi vnT + 2\pi v\tau + \theta)]. \tag{21}$$

It is easily seen that $(-1)^n x(nT + \tau)$ is a single tone. The frequency and phase of the tone could be estimated by the ML estimator proposed in [20]. The detailed algorithm is described as follows.

Letting

$$y(n, \varepsilon) = (-1)^n x(nT + \varepsilon), \tag{22}$$

we calculate the Fourier transform of $y(n, \varepsilon)$ as

$$Y(f, \varepsilon) = \sum_{n=0}^{N-1} y(n, \varepsilon)\, e^{-j2\pi fn} \tag{23}$$

When $|Y(f, \varepsilon)|$ reaches the peak, we have $v = f$ and $\tau = \varepsilon$, i.e.,

$$(v, \tau) = \arg\max_{(f,\varepsilon)} |Y(f, \varepsilon)|. \tag{24}$$

After obtaining the frequency and timing offsets, the carrier phase is estimated by

$$\theta = \arg Y(v, \tau) - 2\pi v\tau. \tag{25}$$

The algorithm was firstly proposed in [13], but it is just used for M-CPFSK signals with $h = 1$. However, the algorithm could be used for any full-response CPM signals with $h = 1$, since the sample point property is available for this type of CPM signals. The algorithm is time-consuming, since the peak search is done in the two-variable function, i.e., both the time and frequency domains.

B. SYNCHRONIZATION SCHEME FROM THE MEAN FUNCTION PROPERTY

Considering

$$E\{x(t)\} = e^{j(2\pi vt+\theta)}\mu(t-\tau) \tag{26}$$

we substitute (13) into (26) and obtain

$$E\{x(t)\} = e^{j(2\pi vt+\theta)}\sum_{m=-\infty}^{\infty} c_m e^{jm\pi(t-\tau)/T}. \tag{27}$$

Considering the Fourier transform of $x(t)$ as follows:

$$S(f) = \int_0^{NT} x(t)\, e^{-j2\pi ft}dt \tag{28}$$

we calculate the expectation

$$E\{S(f)\} = \int_0^{NT} E\{x(t)\}\, e^{-j2\pi ft}dt. \tag{29}$$

For $f = v + k/2T$, we substitute (26) into (29) and obtain

$$E\{S(v+k/2T)\} = c_k NT e^{j(\theta-k\pi\tau/T)} \tag{30}$$

Since $|c_{\pm1}| > |c_k|\,(k \neq \pm1)$, we search the maximal two peaks of $|E\{S(f)\}|$, which respond to $f = v \pm 1/2T$, and then we could obtain the frequency offset v. However, the calculation of $E\{S(v+k/2T)\}$ utilizes $E\{x(t)\}$, which is the statistical mean and difficult to obtain. Supposing

$$S_n = \int_{nT}^{(n+1)T} x(t)\, e^{-j2\pi(v+k/2T)t}dt \tag{31}$$

we have

$$\begin{aligned} E\{S_n\} &= \int_{nT}^{(n+1)T} E\{x(t)\}\, e^{-j2\pi(v+k/2T)t}dt \\ &= c_k T e^{j(\theta-k\pi\tau/T)}. \end{aligned} \tag{32}$$

Then we calculate

$$E\{S_n\} \approx \frac{1}{N}\sum_{n=0}^{N-1} S_n = \frac{1}{N}\int_0^{NT} x(t)\, e^{-j2\pi(v+k/2T)t}dt. \tag{33}$$

The left item of (33) is equal to $\frac{1}{N}E\{S(v+k/2T)\}$ and the right of (33) is equal to $\frac{1}{N}S(v+k/2T)$. Therefore, we have

$$E\{S(v+k/2T)\} \approx S(v+k/2T). \tag{34}$$

Obviously, the approximation becomes an equation when N tends to infinity. Therefore, we have

$$\begin{aligned} S(v+1/2T) &= c_1 NT e^{j(\theta-\pi\tau/T)}, \\ S(v-1/2T) &= c_{-1} NT e^{j(\theta+\pi\tau/T)}. \end{aligned}$$

Finally, the estimators are written as

$$\begin{aligned} v &= \arg\max_f \left(|S(f+1/2T)| + |S(f-1/2T)|\right), \\ \tau &= -\frac{T}{2\pi}\arg S(v+1/2T)\, S^*(v-1/2T), \\ \theta &= \frac{1}{2}\arg S(v+1/2T)\, S(v-1/2T). \end{aligned} \tag{35}$$

The algorithm was proposed in [16] and [17]. The algorithm is just searching the frequency domain, so it is more efficient than the last scheme.

C. SYNCHRONIZATION SCHEME FROM THE CORRELATION FUNCTION PROPERTY

Considering

$$R_m(t) = E\left[x(t)\, x^*(t-mT)\right] = e^{j2\pi mvT} r_m(t-\tau) \tag{36}$$

we substitute (19) into (36) and obtain

$$|R_m(t)| = A_0 + 2\sum_{k=1}^{\infty} A_k \cos\frac{2\pi k(t-\tau)}{T}. \tag{37}$$

According to

$$\int_0^T \cos\frac{2\pi k(t-\tau)}{T} e^{-j\frac{2\pi t}{T}}dt = \begin{cases} \frac{T}{2}e^{-j\frac{2\pi\tau}{T}}, & k = 1; \\ 0, & others, \end{cases}$$

the timing offset can be directly extracted from $R_m(t)$ without the frequency offset information as follows:

$$\tau = -\frac{T}{2\pi}\arg\int_0^T |R_m(t)|\, e^{-j\frac{2\pi t}{T}}dt. \tag{38}$$

When the timing offset is obtained, we have

$$R_m(\tau) = (-1)^m e^{j2\pi mvT}\left(A_0 + 2\sum_{k=1}^{\infty} A_k\right). \tag{39}$$

Therefore, the frequency estimator is

$$v = \frac{1}{2\pi T}\arg\left[-R_m(\tau)\, R_{m-1}^*(\tau)\right]. \tag{40}$$

In order to eliminate the noise interference, we combine the information of $R_m(t)$ with all the m values as follows:

$$\begin{aligned} \tau &= -\frac{T}{2\pi}\arg\int_0^T \left[\sum_{m=1}^{M} |R_m(t)|\right] e^{j\frac{2\pi t}{T}}dt, \\ v &= \frac{1}{2\pi MT}\sum_{m=1}^{M}\arg\left[-R_m(\tau)\, R_{m-1}^*(\tau)\right]. \end{aligned} \tag{41}$$

where correlation function $R_m(t)$ is computed on the CPM signal samples as follows:

$$R_m(t) = \frac{1}{N}\int_0^{NT} x(t)\, x^*(t-mT)\, d\tau \tag{42}$$

The algorithm was firstly proposed in [14], but it just considered the case of $R_1(t)$. Then, in [15] all the m values were used and the estimator (41) was provided. In the following

simulation, we use $M = 10$ which is the highest order used in [15]. However, the scheme is proposed for MSK-type signals, and the algorithm converts $h = 1/2$ to $h = 1$ by square operation. Therefore, the algorithm is suitable for the CPM signals with $h = 1$. The algorithm estimates the parameters by the calculation process not the searching process, so it is most efficient among the three schemes.

D. SYNCHRONIZATION SCHEME EXTENDED TO ARBITRARY h VALUES

The three schemes above are designed for the CPM signals with $h = 1$. For arbitrary h values, the phase unwrapping technique can be used to convert the arbitrary h to *1*. For the CPM signal in (1), the phase unwrapping is to obtain the estimated phase

$$\hat{\phi}(t) = Arg[s(t)] + 2k\pi \tag{43}$$

where k is the proper integer. The standard phase unwrapping algorithm in the discrete form can be implemented by Matlab function 'unwrap' [21]. Under noise-free condition, we have

$$\hat{\phi}(t) = \phi(t). \tag{44}$$

Then we construct the new CPM signal with $h = 1$ as follows:

$$\hat{s}(t) = \exp\left[j\hat{\phi}(t)/h\right]. \tag{45}$$

After the phase transform, the three schemes could be used for $\hat{s}(t)$ to estimate the synchronization parameters $\hat{v}$, $\hat{\theta}$ and $\hat{\tau}$. Considering that the real frequency and phase have been enlarged by $1/h$ times in the transform (45), the real frequency and phase are $v = h\hat{v}$ and $\theta = h\hat{\theta}$. The timing offset is not changed in the transform, so the real timing offset is $\tau = \hat{\tau}$.

Above all, the three schemes have been described. In the sample-point (SP) scheme, we search the frequency and time domains, and obtain the frequency and timing offsets simultaneously. In the mean-function (MF) scheme, we search the frequency domain to find the frequency offset, and then calculate the timing offset and carrier phase. In the correlation-function (CF) scheme, we calculate the timing offset directly, and then calculate the frequency offset. Since the searching process is more time-consuming than the calculation process, the CF scheme is most effective in computation complexity. In the next section, we will compare the estimation performances of the three schemes by numerical simulations.

IV. NUMERICAL SIMULATIONS

In this section, we show the simulation results for CPM signals with rectangular (REC) and raised-cosine (RC) frequency pulses. Though the schemes can be used to deal with the M-ary CPM signals, we provide the numerical simulation results for binary CPM.

For the discrete-time implementation, the sampling rate $fs = 4/T$ is used. The estimation interval corresponds to $N = 50$ symbols. The incoming waveform is first fed to a lowpass filter to eliminate out-of-band noise, which is produced by the Matlab filter design function 'fir1'. The order of the filter is *20* and its bandwidth is h/T. There are 2000 Monte Carlo simulations in each figure.

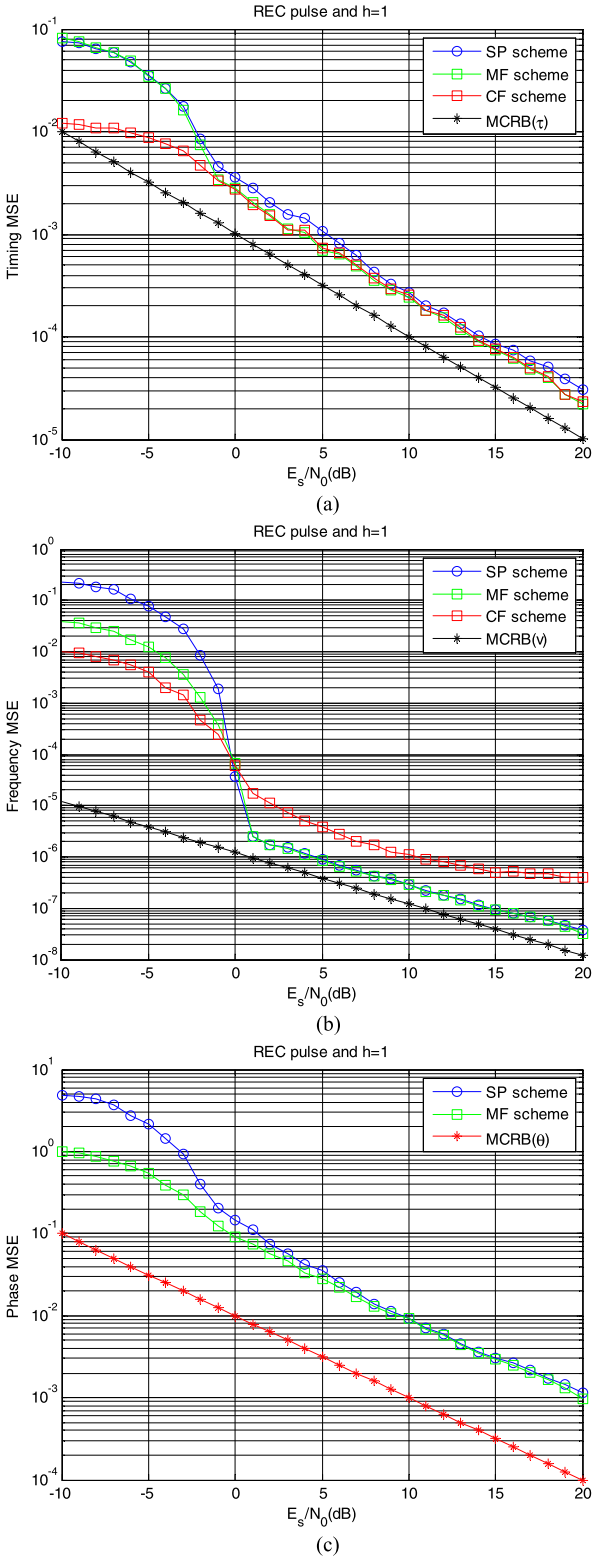

FIGURE 1. Performance comparison for REC pulse and $h = 1$. (a) Timing MSE. (b) Frequency MSE. (c) Phase MSE.

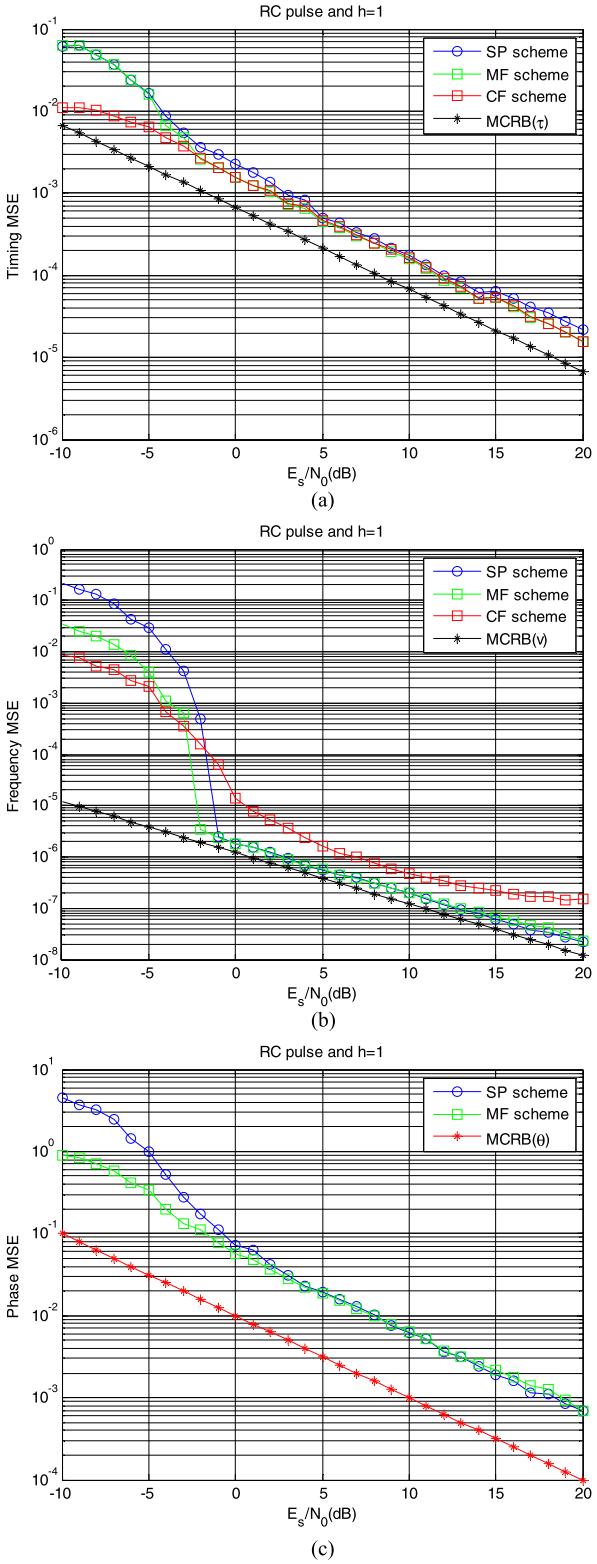

FIGURE 2. Performance comparison for RC pulse and $h = 1$. (a) Timing MSE. (b) Frequency MSE. (c) Phase MSE.

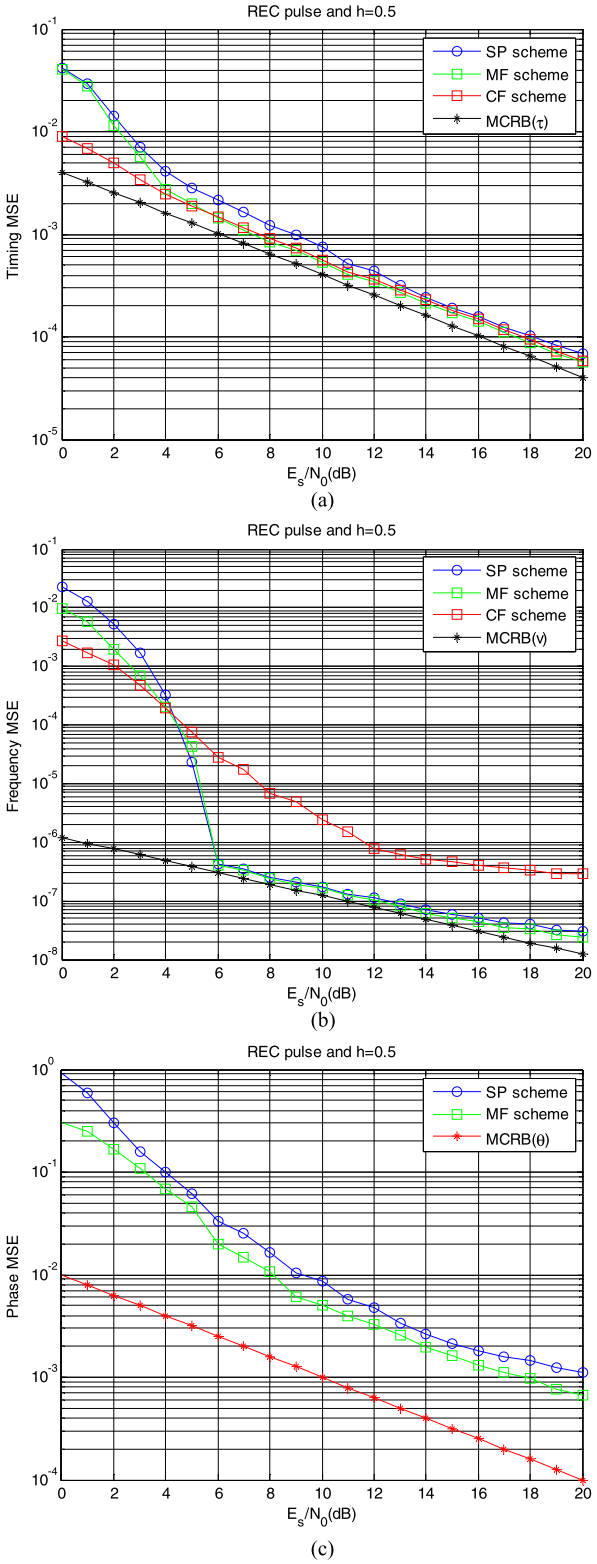

FIGURE 3. Performance comparison for REC pulse and $h = 0.5$. (a) Timing MSE. (b) Frequency MSE. (c) Phase MSE.

The normalized timing, frequency and phase mean square errors (MSEs) as a function of E_s/N_0 are shown in the simulation. Pulse functions and h values are varied from one simulation to another. The tight bounds of the presented three schemes are difficult to obtain, so we just compare the performances with the modified Cramer–Rao bounds (MCRBs),

which are usually used as benchmark in all the available literatures. They are expressed by [3]

$$MCRB(\tau) = \begin{cases} \dfrac{T}{2\pi^2 h^2 N (E_s/N_0)}, & \text{with REC} \\ \dfrac{T}{3\pi^2 h^2 N (E_s/N_0)}, & \text{with RC} \end{cases} \quad (46)$$

$$MCRB(v) = \frac{3}{2\pi^2 T^2 N^3 (E_s/N_0)} \quad (47)$$

$$MCRB(\theta) = \frac{1}{2N (E_s/N_0)} \quad (48)$$

The estimation performances for CPM signals with REC frequency pulse and $h = 1$ are shown in Fig. 1. The three subfigures show the timing, frequency and phase estimation performance. In Fig. 1a, the three schemes have the similar timing performances when the SNR is larger than *0*dB, and the timing MSEs are far from the MCRB about *3*dB. In Fig. 1b, the performances of the SP scheme and the MF scheme are close to the MCRB in high SNR, but the performance of the RF scheme is far from the MCRB. Since the RF scheme calculates the frequency offset using the estimated timing information, the error of the timing increases the error of the frequency estimation. Fig. 1c shows the phase MSEs of the SP and MF schemes, and the RF scheme cannot estimate the carrier phase, since the correlation function does not include the carrier phase information. The performance of the MF scheme is better than that of the SP scheme in low SNR.

The estimation performances for CPM signals with RC frequency pulse and $h = 1$ are shown in Fig. 2. The conclusions are similar to the case with REC pulse. It is because the algorithms are designed for all the full-response CPM signals with $h = 1$ regardless of the pulse type. Since the frequency pulse makes no effect on the estimation performance, we just consider the REC pulse in the following simulation. Now we check the effect of h values on the estimation performance.

Fig. 3 shows the performance for CPM signals with REC pulse and $h = 1/2$. In this case, the phase unwrapping technique is equivalent to the square operation. The SNR threshold of the frequency estimation increases from 1dB ($h = 1$) to 6dB ($h = 1/2$) due to the square operation. However, the timing performance with $h = 1/2$ is closer to the MCRB than that with $h = 1$. It is because the MCRB increases with the decrease of h value. Moreover, the decrease of the bandwidth of the pre-filter also reduces the noise.

Fig. 4 shows the performances for CPM signals with REC pulse and $h = 0.6$. Obviously, the SNR threshold increases from 6dB to 11dB. Only when the SNR is larger than 11dB, the estimation performances are close to the MCRB. It is because phase unwrapping for general cases may encounter the phase ambiguity of 2π in low SNR [21].

In Figs. 1-4, the simulation results indicate that all the three schemes can provide the synchronization parameters for full-response CPM signals with arbitrary h values. However, the MF scheme is better than RF scheme in frequency estimation,

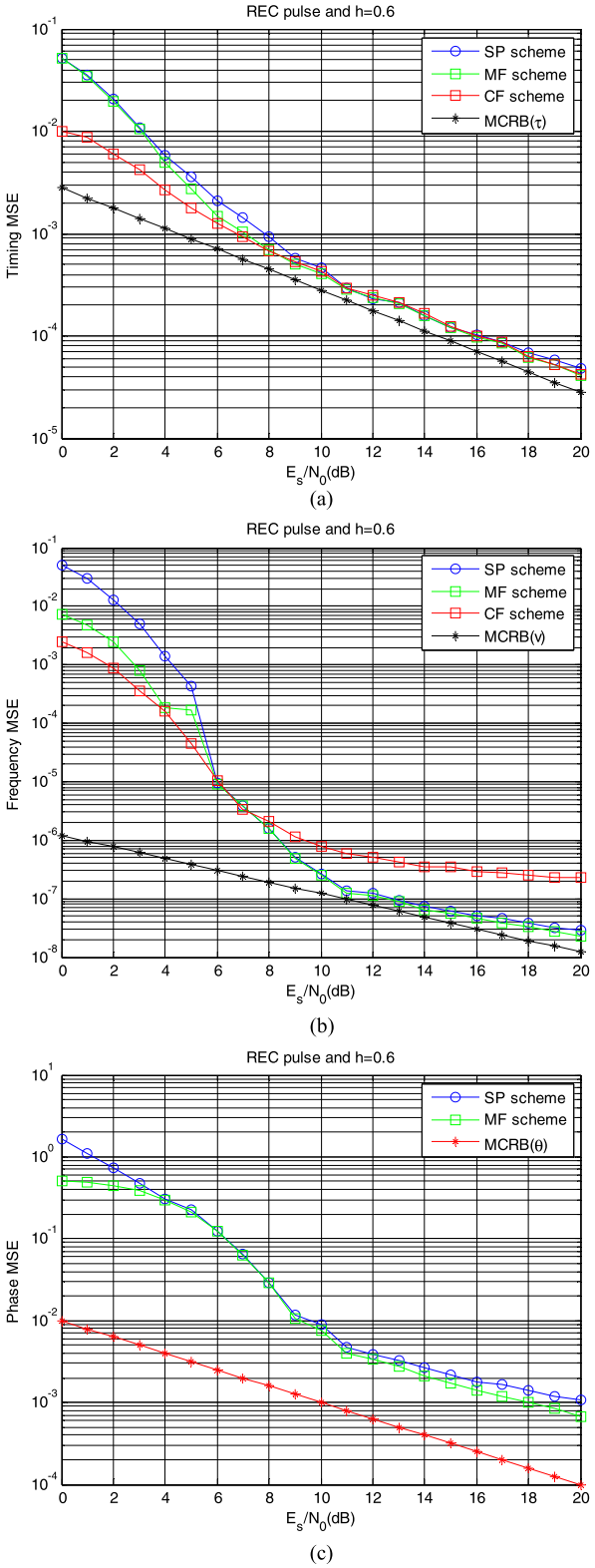

FIGURE 4. Performance comparison for REC pulse and $h = 0.6$. (a) Timing MSE. (b) Frequency MSE. (c) Phase MSE.

and better than SP scheme in phase estimation. Therefore, the MF scheme has the best performance among the three schemes.

V. CONCLUSION

In the paper, we summarize the joint frequency and timing recovery schemes in the available literatures and conclude three statistical characteristics for binary full-response CPM signals with $h = 1$ and arbitrary frequency pulses.

Based on the three properties, the three synchronization schemes are provided in the unified framework and extended to full-response CPM signals with arbitrary h values by phase unwrapping technique. The performances of the three schemes are compared in the numerical simulations and the mean-function scheme shows the best performance.

REFERENCES

[1] A. Barbieri, D. Fertonani, and G. Colavolpe, "Spectrally-efficient continuous phase modulations," *IEEE Trans. Wireless Commun.*, vol. 8, no. 3, pp. 1564–1572, Mar. 2009.

[2] J. B. Anderson, T. Aulin, and C. E. Sundberg, *Digital Phase Modulation*. New York, NY, USA: Plenum, 1986.

[3] U. Mengali and A. N. D'Andrea, *Synchronization Techniques for Digital Receivers*. New York, NY, USA: Plenum, 1997.

[4] J. Huber and W. Liu, "Data-aided synchronization of coherent CPM-receivers," *IEEE Trans. Commun.*, vol. 40, no. 1, pp. 178–189, Jan. 1992.

[5] E. Hosseini and E. Perrins, "Timing, carrier, and frame synchronization of burst-mode CPM," *IEEE Trans. Commun.*, vol. 61, no. 12, pp. 5125–5138, Dec. 2013.

[6] A. N. D'Andrea, U. Mengali, and R. Reggiannini, "The modified Cramer–Rao bound and its application to synchronization problems," *IEEE Trans. Commun.*, vol. 42, no. 324, pp. 1391–1399, Feb./Apr. 1994.

[7] M. Morelli and U. Mengali, "Feedforward carrier frequency estimation with MSK-type signals," *IEEE Commun. Lett.*, vol. 2, no. 8, pp. 235–237, Aug. 1998.

[8] A. N. D'Andrea, U. Mengali, and M. Morelli, "Symbol timing estimation with CPM modulation," *IEEE Trans. Commun.*, vol. 44, no. 10 pp. 1362–1372, Oct. 1996.

[9] M. Morelli, U. Mengali, and G. M. Vitetta, "Joint phase and timing recovery with CPM signals," *IEEE Trans. Commun.*, vol. 45, no. 7, pp. 867–876, Jul. 1997.

[10] Q. Zhao and G. L. Stuber, "Robust time and phase synchronization for continuous phase modulation," *IEEE Trans. Commun.*, vol. 54, no. 10, pp. 1857–1869, Oct. 2006.

[11] A. N. D'Andrea, A. Ginesi, and U. Mengali, "Frequency detectors for CPM Signals," *IEEE Trans. Commun.*, vol. 43, no. 234, pp. 1828–1837, Feb./Apr. 1995.

[12] P. Laurent, "Exact and approximate construction of digital phase modulations by superposition of amplitude modulated pulses (AMP)," *IEEE Trans. Commun.*, vol. COM-34, no. 2, pp. 150–160, Feb. 1986.

[13] G. Caire and C. Elia, "A new symbol timing and carrier frequency offset estimation algorithm for noncoherent orthogonal M-CPFSK," *IEEE Trans. Commun.*, vol. 45, no. 10, pp. 1314–1326, Oct. 1997.

[14] R. Mehlan, Y.-E. Chen, and H. Meyr, "A fully digital feedforward MSK demodulator with joint frequency offset and symbol timing estimation for burst mode mobile radio," *IEEE Trans. Veh. Technol.*, vol. 42, no. 4, pp. 434–443, Nov. 1993.

[15] M. Morelli and U. Mengali, "Joint frequency and timing recovery for MSK-type modulation," *IEEE Trans. Commun.*, vol. 47, no. 6, pp. 938–946, Jun. 1999.

[16] P. Bianchi, P. Loubaton, and F. Sirven, "On the blind estimation of the parameters of continuous phase modulated signals," *IEEE J. Sel. Areas Commun.*, vol. 23, no. 5, pp. 944–962, May 2005.

[17] X. Xie and Z. Xu, "Feedforward joint frequency and timing estimation scheme for M-CPFSK signals," *Electron. Lett.*, vol. 52, no. 10, pp. 876–877, Apr. 2016.

[18] A. Napolitano and C. M. Spooner, "Cyclic spectral analysis of continuous-phase modulated signals," *IEEE Trans. Signal Process.*, vol. 49, no. 1, pp. 30–44, Jan. 2001.

[19] T. Aulin and C. E. Sundberg, "Continuous phase modulation—Part I: F ull response signaling," *IEEE Trans. Commun.*, vol. COM-29, no. 3, pp. 196–209, Mar. 1981.

[20] D. C. Rife and R. R. Boorstyn, "Single tone parameter estimation from discrete-time observations," *IEEE Trans. Inf. Theory*, vol. IT-20, no. 5, pp. 591–598, Sep. 1974.

[21] Z. Xu, B. Huang, and S. Xu, "Robust phase unwrapping algorithm," *Electron. Lett.*, vol. 49, no. 24, pp. 1565–1567, Nov. 2013.

XU XIE (M'09) was born in Wuhan, China, in 1982. He received the M.S. and Ph.D. degrees in communication engineering from the Huazhong University of Science and Technology, Wuhan, in 2010, respectively. He is currently a Lecturer with the Department of Electronics and Engineering, Naval University of Engineering. His teaching duties include graduate and undergraduate-level courses on radio frequency signal processing and wireless communication theory. He has authored several IEEE journal papers, all of them in the area of radio frequency and communication systems. His research interests are centered upon the application of communication signal processing and radio frequency circuit design.

ZHENGGUANG XU was born in Wuhan, China, in 1981. He received the M.S. and Ph.D. degrees in communication engineering from the Huazhong University of Science and Technology, Wuhan, in 2009. He is currently a Lecturer with the College of Electronics and Communications, Huazhong University of Science and Technology. His research interests include signal processing and information hiding.